Reentrant Charge Order Transition in the Extended Hubbard Model

R. Pietig, R. Bulla,* and S. Blawid
Max-Planck-Institut für Physik komplexer Systeme, Nöthnitzer Strasse 38, 01187 Dresden, Germany
(Received 18 December 1998)

We study the extended Hubbard model with both on-site and nearest neighbor Coulomb repulsion (U and V, respectively) in the dynamical mean field theory. At quarter filling, the model shows a transition to a charge ordered phase with different sublattice occupancies $n_A \neq n_B$. The effective mass increases drastically at the critical V and a pseudogap opens in the single-particle spectral function for higher values of V. The $V_c(T)$ curve has a negative slope for small temperatures, i.e., the charge ordering transition can be driven by increasing the temperature. This is due to the higher spin entropy of the charge ordered phase. [S0031-9007(99)09148-6]

PACS numbers: 71.10.Fd, 71.27.+a, 71.45.Lr

The possibility of crystallization of electrons due to their long-range Coulomb repulsion was first proposed by Wigner [1]. He considered an electron system in a uniform positive background at sufficiently low densities. The Wigner lattice is formed when the gain in Coulomb energy due to the localization of the electrons exceeds the gain in kinetic energy for the homogeneous electron distribution. It is experimentally realized in the two dimensional electron gas in a GaAs/AlGaAs heterostructure [2]. Because of the reduced dimensionality, the effect of the Coulomb interaction is enhanced so that the transition to the ordered state occurs at experimentally accessible electron densities.

Crystallization of charge carriers (charge ordering) can also be observed in three dimensional systems, even at very high densities [3]. Here the kinetic energy of the electrons or holes has to be reduced drastically for the charge ordered state to become possible. In 4f-electron systems it is the small hybridization of the well localized 4f orbitals that leads to a reduced kinetic energy. An example is Yb_4As_3 where a first order charge ordering transition occurs at $T_c \approx 295$ K [4,5]. The carrier concentration in Yb_4As_3 (approximately one hole per four Yb ions) is considerably larger than typical values for a Wigner lattice. The kinetic energy of the electrons can also be reduced by the interaction with lattice and spin degrees of freedom. An interplay of these mechanisms is responsible for the charge order transition occurring in a variety of rare earth manganites (e.g., in $La_{1-x}Ca_xMnO_3$ for $x \geq 0.5$ [6]).

In all examples mentioned so far, the charge ordered phase is the ground state. However, a melting of the charge ordered state on *decreasing* the temperature (i.e., a reentrant transition) has been found recently in $Pr_{0.65}(Ca_{0.7}Sr_{0.3})_{0.35}MnO_3$ [7] and in $LaSr_2Mn_2O_7$ [8].

In this Letter, we investigate the simplest model which allows for a charge ordering transition due to the competition between kinetic and Coulomb energy. The extended Hubbard model [9]

$$H = t \sum_{\langle ij\rangle\sigma} (c^\dagger_{i\sigma} c_{j\sigma} + c^\dagger_{j\sigma} c_{i\sigma}) - \mu \sum_{i\sigma} c^\dagger_{i\sigma} c_{i\sigma} + U \sum_i n_{i\uparrow} n_{i\downarrow} + V \sum_{\langle ij\rangle} n_i n_j \quad (1)$$

describes fermions on a lattice with an on-site Coulomb repulsion U, a nearest neighbor Coulomb repulsion V, and a hopping matrix element t. The $c^\dagger_{i\sigma}$ ($c_{i\sigma}$) denote creation (annihilation) operators for a fermion at site i with spin σ, the n_i are defined as $n_i = n_{i\uparrow} + n_{i\downarrow}$ where $n_{i\sigma} = c^\dagger_{i\sigma} c_{i\sigma}$, and $\sum_{\langle ij\rangle}$ indicates the sum over nearest neighbors.

In the following we study the extended Hubbard model Eq. (1) within the dynamical mean field theory (DMFT) [10,11], i.e., in the limit of infinite lattice coordination number z. In order to define a nontrivial limit as $z \to \infty$, the parameters t and V are rescaled as $t \to t/\sqrt{z}$ and $V \to 2V/z$. This leads to a drastic simplification of the self-energy diagrams. The self-energy becomes local and, in particular, the nonlocal Coulomb term contributes only at the Hartree level, i.e., the V term simply acts as a shift of the chemical potential [12]. Therefore, the Hamiltonian

$$H = \sum_{i\sigma} \left(V \sum_j{}' \langle n_j \rangle - \mu \right) c^\dagger_{i\sigma} c_{i\sigma} + t \sum_{\langle ij\rangle\sigma} (c^\dagger_{i\sigma} c_{j\sigma} + c^\dagger_{j\sigma} c_{i\sigma}) + U \sum_i c^\dagger_{i\uparrow} c_{i\uparrow} c^\dagger_{i\downarrow} c_{i\downarrow} \quad (2)$$

($\sum'_j$ indicates the sum over the nearest neighbors of i) leads to the same $z \to \infty$ limit as Eq. (1) after rescaling t and V.

As we are interested in charge ordered phases with different occupancies on the two sublattices A and B of a bipartite lattice, we have to generalize the DMFT equations to allow for solutions with $n_A \neq n_B$. For this, the model (2) is mapped self-consistently on two Anderson impurity models (one for sublattice A and one for sublattice B). In the Bethe lattice case, where the density of states is given by $D(\epsilon) = \frac{2}{\pi W^2}\sqrt{W^2 - \epsilon^2}$ (we set $W = 1$ as the unit for the energy scale), the

 0031-9007/99/82(20)/4046(4)$15.00

self-consistency equations simplify to the form

$$\epsilon_d^{\mathrm{A}} + \Delta_{\mathrm{A}}(i\omega_n) = 2Vn_{\mathrm{B}} - \mu + \frac{W^2}{4} G_{\mathrm{B}}(i\omega_n), \quad (3)$$

$$\epsilon_d^{\mathrm{B}} + \Delta_{\mathrm{B}}(i\omega_n) = 2Vn_{\mathrm{A}} - \mu + \frac{W^2}{4} G_{\mathrm{A}}(i\omega_n). \quad (4)$$

[$G_{\mathrm{A/B}}(i\omega_n)$ are the Green functions for the A/B sublattice and $\Delta_{\mathrm{A/B}}(i\omega_n)$ are the hybridization functions between impurity and the effective conduction band; $n_{\mathrm{A/B}}$ denote the sublattice occupancies and $\epsilon_d^{\mathrm{A/B}}$ are the on-site energies of the effective impurities].

The remaining problem is the iterative solution (i.e., the calculation of the Green functions) of an effective single impurity Anderson model. We use three different methods, an exact diagonalization (ED) technique for finite temperatures, the noncrossing approximation (NCA), and the numerical renormalization group (NRG) method. The ED method diagonalizes an impurity model with a finite number N of conduction band orbitals. Within the self-consistency procedure we define the mapping of the full Green functions $G_{\mathrm{A/B}}(i\omega_n)$ to the hybridization functions $\Delta_{\mathrm{B/A}}(i\omega_n)$ by expanding both sides of (3) and (4) in powers of $(i\omega_n)^{-1}$ and match coefficients up to the order of $(i\omega_n)^{-2N}$. This approximation is similar in spirit to the projection method based on the continued fraction representation used for $T = 0$ [11]. The NRG is applied here for the first time to a particle-hole asymmetric problem within the DMFT. The method is an extension of earlier work on the (not extended) symmetric Hubbard model [13]. Details of the NCA approach are summarized in [14].

Figure 1 shows the (T-V)-phase diagram for $U = 2$ and quarter filling. The results of the different methods agree remarkably well in their corresponding range of applicability. For high temperatures ($T > 0.4$), the ED results for $N = 5$ shown in Fig. 1 can already be obtained from an $N = 3$ calculation (within numerical accuracy). The ED method cannot be used for very low temperatures since only a small number of orbitals is taken into account. The NCA is applicable down to much lower temperatures and we find that the slope of the $V_{\mathrm{c}}(T)$ curve changes its sign at $T \approx 0.1$. The NCA encounters problems in the very low temperature limit. Nevertheless, the extrapolation of the $V_{\mathrm{c}}(T)$ curve to $T = 0$ agrees well with the critical V obtained from the NRG method $V_{\mathrm{c}}(T = 0) \approx 0.66$.

The reentrant behavior in the interval $0.47 < V < 0.66$ is due to the higher spin entropy of the charge ordered state. As we have neglected the possibility of an additional magnetic ordering in the charge ordered state, the contribution of the spin degrees of freedom to the entropy is approximately ln(2) per occupied site. The entropy of the homogeneous phase, which is a Fermi liquid, grows linearly with T. On further increasing the temperature, the increasing charge entropy of the homogeneous phase dominates and the system shows the usual melting behavior.

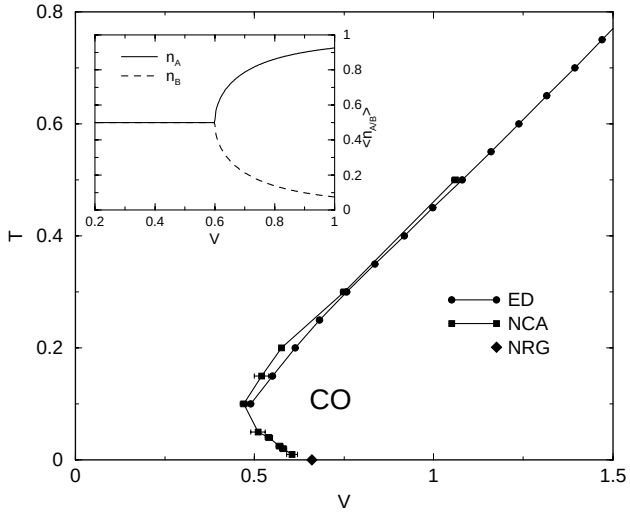

FIG. 1. Phase diagram for the extended Hubbard model ($U = 2$, quarter filling). The various symbols show the results for the phase boundary between the homogeneous and the charge ordered phase (CO) from ED (circles), NCA (squares), and NRG calculations (diamond). The inset shows the ED result for the V dependence of the lattice occupancies for $U = 2$ and $T = 0.2$.

The inset of Fig. 1 shows the ED result for the V dependence of the sublattice occupancies n_{A} and n_{B} ($T = 0.2, U = 2$). The transition is clearly continuous, in contrast to the result for $T = 0$ where the NRG gives a first order phase transition with a jump in the order parameter $\delta n = n_{\mathrm{A}} - n_{\mathrm{B}}$ from 0 to $\delta n \approx 0.7$. Unfortunately, it is not possible to clarify numerically how the first order transition at $T = 0$ evolves from the continuous transition at finite T. There are numerical indications that δn increases more rapidly at the transition when T is reduced. However, the convergence of the iterative procedure is extremely slow near the phase boundary.

The NRG results for the A and B spectral functions for $T = 0$ are shown in Fig. 2. Below $V = V_{\mathrm{c}}$, the A and B spectral functions are equal and independent of V (the extended Hubbard model in the DMFT reduces to the ordinary Hubbard model as long as the homogeneous phase is considered; the solution shown in Fig. 2 for $V = 0.65$ is therefore also the solution for the Hubbard model with $V = 0$). The discontinuous transition to a finite δn at V_{c} is reflected in a redistribution of spectral weight in the spectral functions above V_{c}.

For $V = 0.665$ the system is still a Fermi liquid with a strongly enhanced effective mass ($m^*/m \approx 120$) and a very narrow quasiparticle resonance at the Fermi level. The effective mass increases further on increasing V and an extreme narrow quasiparticle resonance is still present for $V = 1.5$ (the width of this resonance is below the energy resolution used in Fig. 2 so that the peak

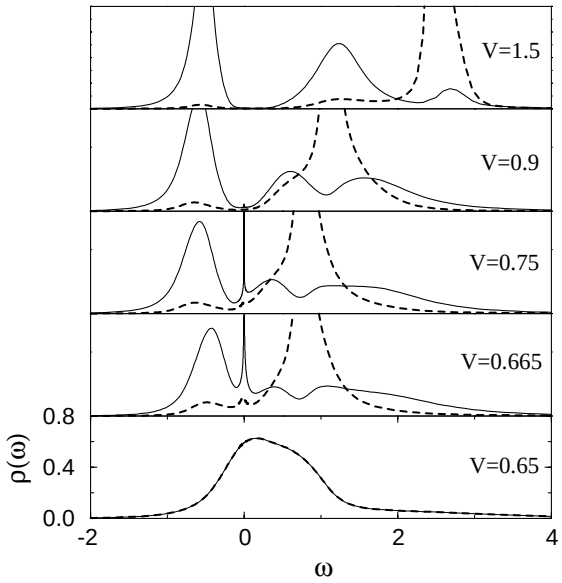

FIG. 2. NRG results for the A and B spectral functions $\rho(\omega)$ (solid and dashed lines, respectively) for $U = 2$, $T = 0$, and different values of V. Below the critical $V_c \approx 0.66$, the spectral functions of both sublattices are equal.

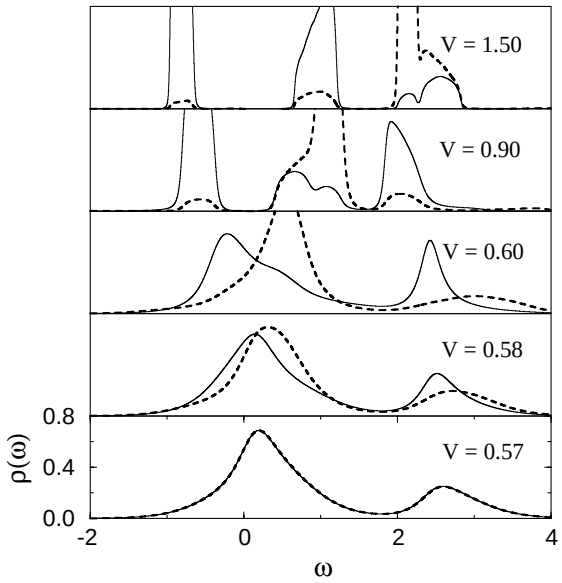

FIG. 3. NCA results for the A and B spectral functions $\rho(\omega)$ (solid and dashed lines, respectively) $U = 2$, $T = 0.2$, and different values of V. For $V \geq 0.58$ charge order sets in and a pseudogap develops at the Fermi level.

is not visible). The quasiparticle resonance vanishes in the limit $V \to \infty$. Although the system is still a Fermi liquid on an extremely small energy scale, a pseudogap in the A and B spectral functions gradually develops at $V \approx 0.9$. The spectral weight within the pseudogap decreases approximately as $1/V^2$ for large V.

The NCA result for the spectral function for $U = 2$, $T = 0.2$, and various values of V is shown in Fig. 3. The very narrow quasiparticle peak seen at $T = 0$ is absent because the temperature exceeds the low-energy scale associated with the Fermi liquid behavior. In contrast to the $T = 0$ case, the transition is continuous which is reflected in the continuous transfer of spectral weight at the transition. A comparison of the NRG and NCA results for $V = 0.9$ and $V = 1.5$ shows a good agreement of the main features of the spectral functions. However, the resolution of the high-energy features is limited in the NRG since the spectra are obtained by broadening a discrete set of δ peaks.

In the homogeneous phase, the NCA spectral function shows the splitting in the upper and lower Hubbard band. The weight of the upper Hubbard band in the B-spectral function is considerably larger compared to the NRG result for $T = 0$. The weight decreases on increasing V in the charge ordered phase because the occupancy of the B sites is suppressed. In addition, the bands in the spectral function narrow due to the reduced hopping of the electrons in the charge ordered phase. In the limit of large V, perfect charge order evolves ($n_A \to 1$ and $n_B \to 0$). Therefore, in this limit the total spectral function of the extended Hubbard model has a simple three-peak structure with peaks at $E_1 = -\mu$, $E_2 = U - \mu$, and $E_3 = 2V - \mu$. The peak at E_1 corresponds to the process of taking out one electron from an (singly occupied) A site, the peak at E_2 is due to the addition of an electron to an A site, and the peak at E_3 comes from the addition of an electron to a B site.

It is tempting to explain the opening of the charge order gap by the change of the unit cell alone, reflecting the broken AB symmetry of the lattice. Although the AB symmetry is, of course, broken at the charge order transition, our results for the spectral function cannot be understood within a one-particle picture. First of all, the charge order gap visible in the spectral function is not a real hard gap but only a pseudogap (i.e., an energy regime of strongly reduced spectral weight) even at zero temperature. From an experimental point of view this difference is irrelevant. However, a pseudogap cannot be obtained by a simple band splitting due to a reduced symmetry. To demonstrate the many-particle character of the bands, we have doped the extended Hubbard model away from quarter filling (see Fig. 4). Note that within our approach the charge ordered state on the A/B sublattice exists also for $n \neq 1$. A rapid weight transfer between the high- and the low-energy scale is observed, which is a characteristic feature of strongly correlated electron systems. A well examined example is the usual half filled Hubbard model, where the weight of the lower Hubbard band decreases faster than the doping x [15,16]. In the extended Hubbard model we find the same behavior.

In conclusion, we have found that the charge order transition in the infinite dimensional extended Hubbard model shows a number of very interesting features. For low temperatures, the system is a Fermi liquid for *both* $V < V_c$ and $V > V_c$. Nevertheless, the effective

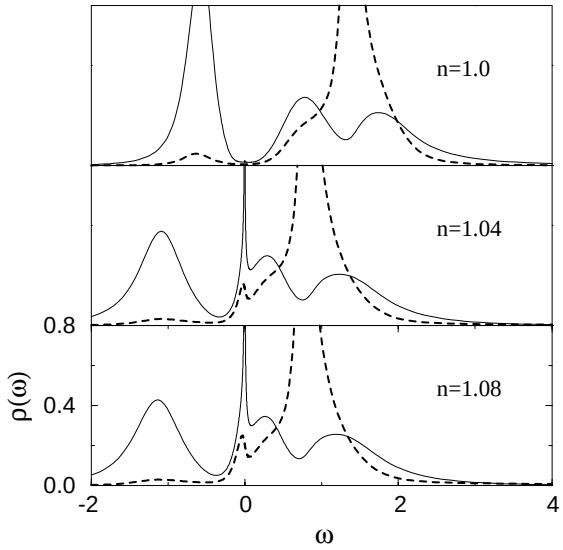

FIG. 4. NRG results for the A and B spectral functions $\rho(\omega)$ (solid and dashed lines, respectively) for $V = 1.0$, $T = 0$, $U = 2$, and different occupancies n. A transfer of weight from the lower Hubbard band (of both A and B spectral functions) to the Fermi level is clearly visible.

mass undergoes a rapid change at the transition. The corresponding very narrow quasiparticle peak at the Fermi energy will hardly be seen in photoemission experiments of charge ordered materials. However, the huge mass enhancement at the transition has drastic consequences on the transport properties, e.g., on the resistivity. This is the case in Yb_4As_3, where the charge order transition is accompanied by a jump in the resistivity.

In our model calculations, we find a real first order transition only for $T = 0$, although the transition remains sharp also for small $T \neq 0$. The occurrence of a first order transition at *finite* temperatures in the above mentioned examples indicates that lattice degrees of freedom are involved. Indeed, the charge order transition in Yb_4As_3 is accompanied by a structural phase transition.

For a particular range of the nearest neighbor Coulomb repulsion V the extended Hubbard model shows reentrant behavior, i.e., a transition from the charge ordered to the homogeneous phase with *decreasing* temperature. This behavior is experimentally seen in $Pr_{0.65}(Ca_{0.7}Sr_{0.3})_{0.35}MnO_3$ [7] and in $LaSr_2Mn_2O_7$ [8]. Moreover, the bandwidth in $Pr_{0.65}(Ca_{1-y}Sr_y)_{0.35}MnO_3$ can be varied by doping with Sr or by applying a magnetic field. For sufficiently small kinetic energy of the electrons only one charge order transition occurs. Increasing the kinetic energy, a reentrant regime is found until for high dopings or magnetic fields the charge order is totally suppressed. Although the localization mechanisms in the rare-earth manganites are more complex than the one induced by a nearest neighbor Coulomb repulsion, we find the same behavior in our model as a function of V/W. We take this as an indication that the occurrence of a reentrant charge order transition does not depend on details of the localization mechanism.

Finally, in photoemission experiments of charge ordered materials the many-particle character of the system should be seen in a weight transfer upon doping with additional charges.

The authors would like to thank P. van Dongen and P. Thalmeier for helpful discussions.

*Present address: Theoretische Physik III, Elektronische Korrelationen und Magnetismus, Universität Augsburg, D-86135 Augsburg, Germany.

[1] E. Wigner, Trans. Faraday Soc. **34**, 678 (1938).
[2] E. Y. Andrei, G. Deville, D. C. Glattli, F. I. B. Williams, E. Paris, and B. Etienne, Phys. Rev. Lett. **60**, 2765 (1988); I. V. Kukushkin, N. J. Pulsford, K. v. Klitzing, R. J. Haug, K. Ploog, and V. B. Timofeev, Europhys. Lett. **23**, 211 (1993).
[3] P. Fulde, Ann. Phys. (Leipzig) **6**, 178 (1997).
[4] A. Ochiai, T. Suzuki, and T. Kasuya, J. Phys. Soc. Jpn. **59**, 4129 (1990); M. Kohgi, K. Iwasa, A. Ochiai, T. Suzuki, J.-M. Mignot, B. Gillon, A. Gukasov, J. Schweizer, K. Kakurai, M. Nishi, A. Dönni, and T. Osakabe, Physica (Amsterdam) **230B–232B**, 638 (1997); M. Rams, K. Kólas, K. Tomala, A. Ochiai, and T. Suzuki, Hyperfine Interact. **97–98**, 125 (1996).
[5] P. Fulde, B. Schmidt, and P. Thalmeier, Europhys. Lett. **31**, 323 (1995).
[6] C. H. Chen and S.-W. Cheong, Phys. Rev. Lett. **76**, 4042 (1996); S. Mori, C. H. Chen, and S.-W. Cheong, Nature (London) **392**, 473 (1998).
[7] Y. Tomioka, A. Asamitsu, H. Kuwahara, and Y. Tokurai, J. Phys. Soc. Jpn. **66**, 302 (1997).
[8] T. Kimura, R. Kumai, Y. Tokura, J. Q. Li, and Y. Matsui, Phys. Rev. B **58**, 11 081 (1998).
[9] R. Micnas, J. Ranninger, and S. Robaszkiewicz, Rev. Mod. Phys. **62**, 113 (1990); K. Penc and F. Mila, Phys. Rev. B **49**, 9670 (1994); P. G. J. van Dongen, Phys. Rev. Lett. **74**, 182 (1995).
[10] W. Metzner and D. Vollhardt, Phys. Rev. Lett. **62**, 324 (1989).
[11] A. Georges, G. Kotliar, W. Krauth, and M. J. Rozenberg, Rev. Mod. Phys. **68**, 13 (1996).
[12] E. Müller-Hartmann, Z. Phys. B **74**, 507 (1989).
[13] R. Bulla, A. C. Hewson, and Th. Pruschke, J. Phys. Condens. Matter **10**, 8365 (1998).
[14] S. Blawid, Phys. Rev. B **59**, 4777 (1999).
[15] A. Harris and R. Lange, Phys. Rev. **157**, 295 (1967).
[16] H. Eskes and A. Oleś, Phys. Rev. Lett. **73**, 1279 (1994).